© 2021. Published by The Company of Biologists Ltd | Development (2021) 148, dev199780. doi:10.1242/dev.199780

RESEARCH ARTICLE

Duplicated antagonistic EPF peptides optimize grass stomatal initiation

Raman Jangra[1], Sabrina C. Brunetti[1], Xutong Wang[1,2], Pooja Kaushik[1], Patrick J. Gulick[1], Nora A. Foroud[3], Shucai Wang[4] and Jin Suk Lee[1,*]

ABSTRACT

Peptide signaling has emerged as a key component of plant growth and development, including stomatal patterning, which is crucial for plant productivity and survival. Although exciting progress has been made in understanding EPIDERMAL PATTERNING FACTOR (EPF) signaling in *Arabidopsis*, the mechanisms by which EPF peptides control different stomatal patterns and morphologies in grasses are poorly understood. Here, by examining expression patterns, overexpression transgenics and cross-species complementation, the antagonistic stomatal ligands orthologous to *Arabidopsis* AtEPF2 and AtSTOMAGEN/AtEPFL9 peptides were identified in *Triticum aestivum* (wheat) and the grass model organism *Brachypodium distachyon*. Application of bioactive BdEPF2 peptides inhibited stomatal initiation, but not the progression or differentiation of stomatal precursors in *Brachypodium*. Additionally, the inhibitory roles of these EPF peptides during grass stomatal development were suppressed by the contrasting positive action of the BdSTOMAGEN peptide in a dose-dependent manner. These results not only demonstrate how conserved EPF peptides that control different stomatal patterns exist in nature, but also suggest new strategies to improve crop yield through the use of plant-derived antagonistic peptides that optimize stomatal density on the plant epidermis.

KEY WORDS: EPF peptides, Stomatal development, Grass, *Brachypodium*

INTRODUCTION

Intercellular signaling mediated by peptide ligands, which are encoded by gene families, plays a central role in plant growth and development, including stomatal patterning. Stomata are valves on the plant epidermis that control water and gas exchange between the plant and the atmosphere. As such, understanding the mechanism by which stomata develop, a process that influences transpiration efficiency and plant biomass production, offers tremendous opportunities to enhance agronomic productivity (Hetherington and Woodward, 2003; Lawson and Blatt, 2014). In *Arabidopsis*, several members of the EPIDERMAL PATTERNING FACTOR (EPF) family of secreted cysteine-rich peptides act as cell-cell signals for stomatal development. AtEPF1 and AtEPF2, the two most closely related peptides among the 11 EPF family members in *Arabidopsis*, are negative regulators of stomatal development. AtEPF1 controls stomatal spacing and differentiation, whereas AtEPF2 inhibits asymmetric cell divisions that initiate the stomatal cell lineage (Hara et al., 2007, 2009; Hunt and Gray, 2009). By contrast, AtSTOMAGEN/AtEPFL9 was identified as a positive regulator of stomatal development, thereby functioning in a completely opposite manner to AtEPF1 and AtEPF2 peptide signaling (Hunt et al., 2010; Kondo et al., 2010; Sugano et al., 2010). Interestingly, two of these opposing stomatal signals, AtEPF2 and AtSTOMAGEN, were identified as endogenous agonistic and antagonistic ligands for the same receptor kinase, ERECTA (ER), to fine-tune stomatal development in *Arabidopsis* (Lee et al., 2015). Other AtEPF family members have also been identified as key signaling molecules controlling other developmental processes, such as the growth of inflorescence (Kosentka et al., 2019; Tameshige et al., 2016; Uchida et al., 2012; Uchida and Tasaka, 2013), highlighting the central importance of *Arabidopsis* EPF peptide signaling in plant growth and development.

Although plants of the grass family provide the majority of the world's food supply, many aspects of their development and physiology are less well understood than those of model dicot species. Stomatal development in grasses differs in many ways from that in *Arabidopsis* (Cai et al., 2017; Chen et al., 2017; Hepworth et al., 2018). For example, unlike the two kidney-shaped guard cells in *Arabidopsis*, the dumbbell-shaped stomatal complexes in grasses are composed of four cells: a pair of guard cells flanked by a pair of subsidiary cells. Additionally, stomata in grasses are arranged linearly in specific cell files next to veins, which are established at the base of young grass leaves, whereas, in most dicots, stomata are dispersed as a result of the formation of scattered stomatal precursors on the epidermis. Thus, one interesting question that arises from this comparison is how different stomatal patterns and morphologies are generated in monocot crops, the answer to which may inform plant-breeding strategies for the improvement of water-use efficiency and crop biomass production. Based on the knowledge of genes regulating stomatal development in the dicot *Arabidopsis*, recent investigations have started to address this important question by identifying their grass homologs. Interestingly, despite different grass stomatal morphologies and patterns, many of the grass homologs of *Arabidopsis* basic helix-loop-helix (bHLH) transcription factors involved in stomatal development have also been shown to control grass stomatal development, although their specific roles have diverged among grass species (Liu et al., 2009; Raissig et al., 2016, 2017;

[1]Department of Biology, Concordia University, Montreal, Quebec, H4B 1R6, Canada. [2]Key Laboratory of Molecular Epigenetics of MOE and Institute of Genetics and Cytology, Northeast Normal University, Changchun 130024, China. [3]Lethbridge Research and Development Centre, Agriculture and Agri-Food Canada, Lethbridge, Alberta, T1J 4B1, Canada. [4]Laboratory of Plant Molecular Genetics & Crop Gene Editing, School of Life Sciences, Linyi University, Linyi 276000, China.

*Author for correspondence (jinsuk.lee@concordia.ca)

R.J., 0000-0001-9792-2818; S.C.B., 0000-0002-6360-4747; X.W., 0000-0001-5765-5671; P.J.G., 0000-0001-7587-4616; N.A.F., 0000-0001-8677-4784; S.W., 0000-0001-7619-2385; J.S.L., 0000-0001-9254-9268

Handling Editor: Ykä Helariutta
Received 7 May 2021; Accepted 19 July 2021

Development (2021) 148, dev199780. doi:10.1242/dev.199780

Wang et al., 2019; Wu et al., 2019). Recently, overexpression of the grass 'AtEPF1' homolog, which is similar in sequence to *Arabidopsis* EPF1 and EPF2, was shown to inhibit stomatal differentiation (Caine et al., 2019; Dunn et al., 2019; Hughes et al., 2017; Lu et al., 2019). In rice, homologs of AtSTOMAGEN promoting stomatal development have also been identified (Lu et al., 2019; Yin et al., 2017), but the existence of grass EPF peptide(s) regulating other aspects of stomatal development and the mechanisms of how each EPF peptide functions to control grass stomatal development remain unknown.

To understand the roles of secreted EPF peptides in grass stomatal development, we searched for entire sets of EPF homologs in the DNA sequence databases for all major cereal crops, as well as for the model grass species *Brachypodium distachyon*. These homologs were characterized by using a combination of bioinformatics, expression analyses and a series of functional genomic studies. We identified four grass EPF homologs of the well-known *Arabidopsis* stomatal EPFs, AtEPF1, AtEPF2 and AtSTOMAGEN, that control grass stomatal development and patterning. Furthermore, using the bioactive *Brachypodium* EPF peptides, which were applied directly to plant seedlings to examine phenotypic responses, we found that these peptides are integral to the initiation of stomatal lineages in *Brachypodium*. This further corroborates that these peptides act as duplicated orthologs of *Arabidopsis* AtEPF2 and AtSTOMAGEN. Our finding emphasizes that, despite plant species-specific differences in stomatal patterning, stomatal initiation in both dicots and grasses depends on a precise balance of closely related EPF peptides with opposing functions.

RESULTS

Identification and expression patterns of the EPF signaling peptide family in grasses

Homologs of the *Arabidopsis* EPF family of signaling peptides were identified in cereal grasses by searching numerous publicly accessible databases of genomic and transcriptomic sequences. The phylogenetic analysis revealed that there are 11-15 genes per haploid genome that encode putative EPFs in each of the six grass species examined (Fig. 1; Fig. S1, Table S1). *Triticum aestivum*,

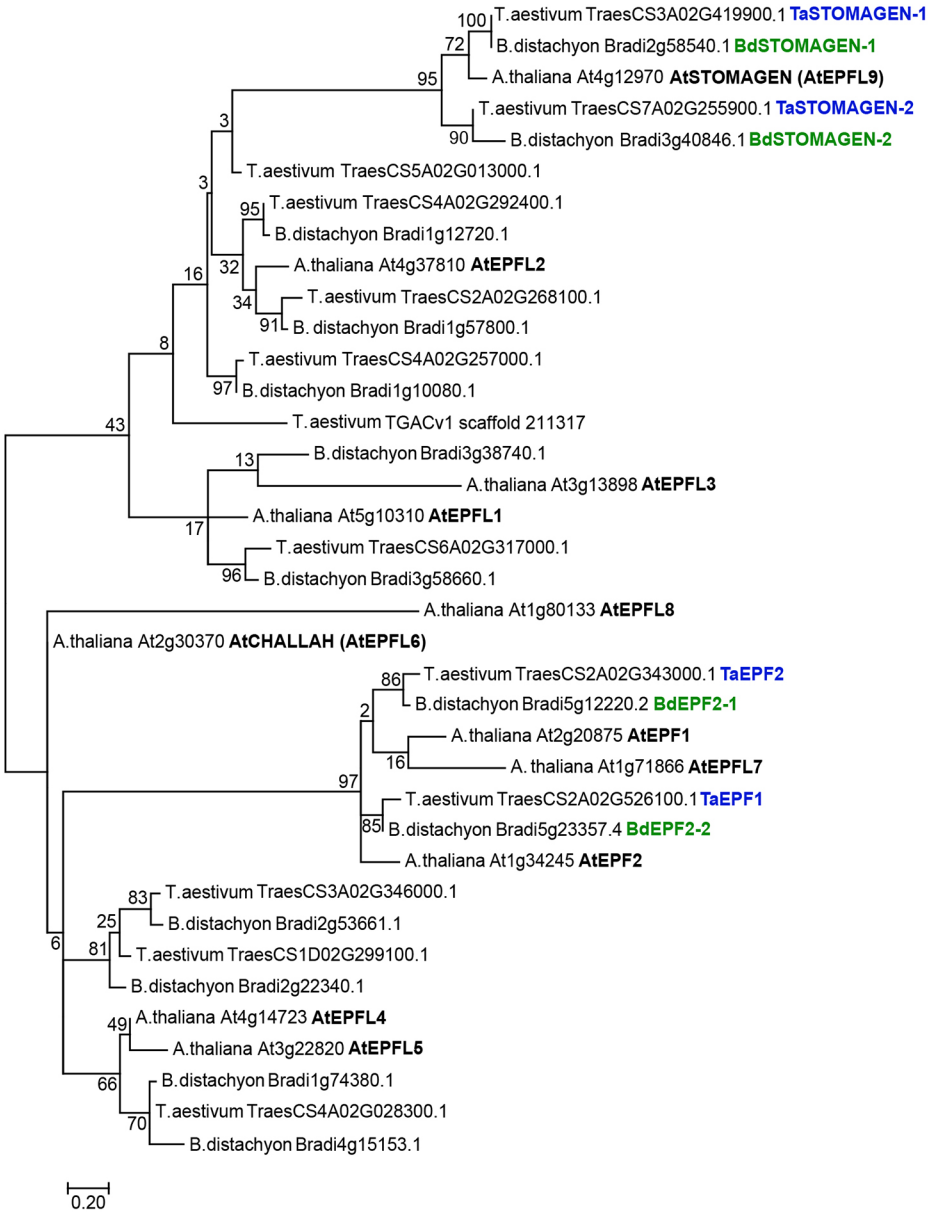

Fig. 1. Identification of grass EPF family peptides. Phylogenetic tree of the EPF family members in *Arabidopsis* (black font), *Brachypodium* (*EPF1*/*EPF2* and *STOMAGEN*-like genes; green font) and wheat (*Triticum aestivum*, *EPF1*/*EPF2* and *STOMAGEN*-like genes; blue font). The tree was constructed in MEGA7 (Kumar et al., 2016) using the amino acid sequences of the predicted mature EPF (MEPF) region of EPF family members and their homologs. The tree is drawn to scale, with branch lengths measured in the number of substitutions per site. MEPF sequence alignment is shown in Fig. S1B.

Development (2021) 148, dev199780. doi:10.1242/dev.199780

which is an allohexaploid species, had 13 paralogous genes, each present with three homeologous gene copies, with the exception of one that had only two homeologs. Of the 38 *EPF*-like genes of *T. aestivum*, 13 were either misannotated or not annotated in the V1 wheat genome assembly at Ensembl Plant, and these were corrected using comparisons to transcriptome databases (Table S2). Gene sequences for *Oryza sativa* and *Sorghum bicolor* EPF genes were taken from a previous report (Takata et al., 2013). The initial sequences included partial-length sequences, which were supplemented with full-length sequences identified in GenBank (GB). Three additional *Oryza* EPF genes were identified in GB databases. Some of the previously described EPF family members were removed from the set used in this study because of low sequence similarity to known EPF genes. Each EPF gene has six conserved cysteines in the predicted mature EPF (MEPF) domain at its C-terminal end (Fig. S1B, Table S3), which are crucial for the biological activity of secreted cysteine-rich peptides, including *Arabidopsis* EPFs. Among the 11 *Arabidopsis* EPF family members, stomatal EPF peptides AtEPF1, AtEPF2 and AtSTOMAGEN are the most well-characterized EPFs. Candidate orthologs of these stomatal EPFs were identified with two *EPF1/EPF2*-like genes, each with high sequence similarity to the C terminus of AtEPF1 and AtEPF2, and two *STOMAGEN*-like genes found in each of the cereal genomes characterized.

To examine the potential role of grass EPF homologs in growth and development, we performed real-time quantitative (q)PCR to analyze the expression patterns of each EPF gene in different organs and developmental stages in the two grass species, wheat (*T. aestivum*) and *Brachypodium* (Fig. 2A,B). In *Brachypodium*, expression of two *EPF1/EPF2*-like (*Bd5g12220* and *Bd5g23357*) and two *STOMAGEN*-like (*Bd2g58540* and *Bd3g40846*) genes, having high sequence similarity to *Arabidopsis* stomatal EPF peptides, was significantly greater in the aerial parts of the plants, including the developing leaves, compared with the roots at both early and late stages of development. Wheat plants also showed similar expression patterns for stomatal EPF homologs, including two *EPF1/EPF2*-like genes (*TraesCS2A02G526100* and *TraesCS2A02G343000*) and two *STOMAGEN*-like genes (*TraesCS3A02G419900* and *TraesCS7A02G255900*), although *TraesCS7A02G255900* transcripts were detected at much lower levels than for *TraesCS3A02G419900*. These expression patterns are consistent with the potential roles of these genes in controlling stomatal development. In a recent overexpression study of *Ta2G556200/TaEPF1B*, one of the three homeologous gene copies of *TraesCS2A02G526100* (hereafter referred to as *TaEPF1*) and *Ta2G343000/TaEPF2D*, one of the three homeologous gene copies of *TraesCS2A02G343000* (hereafter referred to as *TaEPF2*), resulted in decreased stomatal numbers with arrested stomatal precursors, a phenotype similar to the overexpression of *Arabidopsis AtEPF1* (Dunn et al., 2019). In line with previous findings in *Arabidopsis* (Uchida et al., 2012), the grass homologs of *AtEPFL4* and *AtCHALLAH/AtEPFL6* (*Bd1g74380*, *Bd4g15153*, *Bd2g53661*, *Bd2g22340*, *TraesCS1D02G299100*, *TraesCS4A02G028300* and *TraesCS3A02G346000*), which are known to regulate inflorescence growth in *Arabidopsis*, are also expressed in the inflorescence stems of both *Brachypodium* and wheat. This suggests that they may play similar roles in inflorescence development in grasses. Together, these observations provide evidence that these secreted EPF peptides are active in grasses and may have conserved functions in controlling various developmental processes in both dicots and grasses.

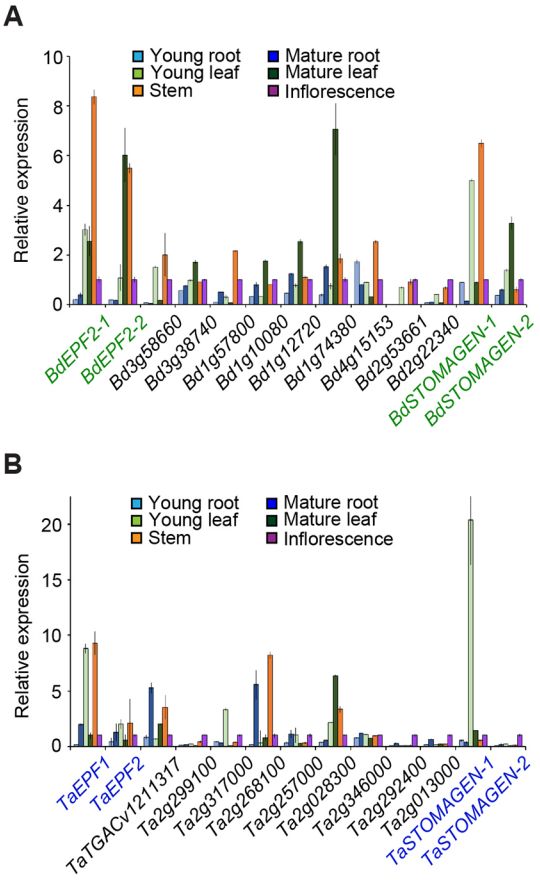

Fig. 2. Expression pattern of EPF family members in *Brachypodium* and wheat. (A) Relative expression levels of EPF homologs (*EPF1*/*EPF2* and *STOMAGEN*-like genes; green font) in different *Brachypodium* tissues: young roots, mature roots, young leaves, mature leaves, stems and inflorescences. Young roots and leaves were obtained from seedlings 5-7 days post germination (dpg). Samples of mature roots, leaves and stems at 10 weeks post germination and inflorescences at 10 days after flowering were used. *BdUBC18* was used as an internal control and the data for inflorescences were set to 1. Data are mean ±s.e. (*n*=3). (B) Relative expression levels of EPF homologs (*EPF1*/*EPF2* and *STOMAGEN*-like genes; blue font) in different wheat tissues: young roots, mature roots, young leaves, mature leaves, stems and inflorescences. Young roots and leaves were obtained from seedlings 3-5 dpg. Mature roots, leaves and stems at 10 weeks post germination and inflorescences at 10 days after flowering were used. *TaRP15* was used as an internal control and the data for inflorescences were set to 1. Data are mean±s.e. (*n*=3).

Overexpression of grass *EPF1*/*EPF2*-like genes restricts the initiation of the stomatal lineage, whereas *STOMAGEN*-like genes promote stomatal development in *Arabidopsis*

Among the family of 11 *Arabidopsis* EPF peptides, stomatal EPFs are the most well-characterized members to date and the biological roles of other EPF peptides remain unknown. Thus, to gain insight into the functional importance and conservation of grass EPF homologs, we conducted further analyses using a subset of grass EPFs that have high sequence similarity to the *Arabidopsis* stomatal EPF peptides. Using an estradiol-induction system, we first generated transgenic *Arabidopsis* plants overexpressing genes from two grass species, wheat and *Brachypodium*, that are homologous to *Arabidopsis* EPF genes controlling stomatal development (Fig. 3; Figs S2, S3). As previously reported, ectopic expression of either of the negative stomatal peptides in *Arabidopsis*, induced overexpression of *AtEPF1* (*iAtEPF1*) and *AtEPF2* (*iAtEPF2*) led to an epidermis devoid of stomata, which resulted in dramatically

Development (2021) 148, dev199780. doi:10.1242/dev.199780

decreased stomatal density (number of stomata per mm^2, Fig. 3A,B,M) and, thus, seedling lethality (Hara et al., 2007, 2009; Hunt and Gray, 2009; Lee et al., 2012). However, consistent with their distinct functions during stomatal development in *Arabidopsis*, overexpression of *AtEPF1* led to an epidermis with arrested stomatal precursors, which resulted in significantly increased nonstomatal cell density (number of nonstomatal epidermal cells per mm^2, Fig. 3A,M,N). By contrast, *AtEPF2* overexpressors displayed an epidermis without any stomatal lineage cells (Fig. 3B,M,N) (Hara et al., 2007, 2009; Hunt and Gray, 2009). Given their high sequence similarity to these two *Arabidopsis* EPF peptides, we speculated that each of the two *EPF1/EPF2*-like genes in wheat and *Brachypodium* would behave in a similar way to their corresponding peptides in *Arabidopsis*, AtEPF1 and AtEPF2, respectively. However, unexpectedly, both of the *EPF1/EPF2*-like genes from *Brachypodium* (*iBd5g12220* and *iBd5g23357*) led to an epidermis completely devoid of all stomatal lineage cells in each of more than 30 T1 or T2 transgenic *Arabidopsis* lines examined for each construct (Fig. 3E,F,M,N; Fig. S2). Likewise, induction of both *iTaEPF1* and *iTaEPF2* overexpression inhibited the entry of cells into the stomatal lineage, a phenotype identical to induced *EPF2* overexpression in *Arabidopsis* (Fig. 3I,J,M,N; Fig. S3). These observations demonstrate that, when expressed in *Arabidopsis*, all grass homologs of *AtEPF1* and *AtEPF2* examined (*Bd5g12220*, *Bd5g23357*, *TaEPF1* and *TaEPF2*) have *Arabidopsis* AtEPF2-like biological activity, which restricts entry asymmetric divisions during stomatal development in *Arabidopsis*, rather than AtEPF1-like activity, which inhibits later stages of development after the initiation of the stomatal lineage. Based on these findings, we named the two *EPF1/EPF2*-like genes (*Bd5g12220* and *Bd5g23357*) from *Brachypodium* as *BdEPF2-1* and *BdEPF2-2*, respectively.

Next, to determine the effects of ectopic expression of grass homologs of *AtSTOMAGEN*, the only positive EPF stomatal signal identified in *Arabidopsis*, we generated transgenic *Arabidopsis* plants overexpressing each of two *STOMAGEN*-like genes from both *Brachypodium* (*Bd2g58540* and *Bd3g40846*) and wheat (*TraesCS3A02G419900* and *TraesCS7A02G255900*) using an estradiol-induction system (Fig. 3; Figs S2, S3). Similar to the effects of *AtSTOMAGEN* overexpression, inducing either copy of the grass homologs of *AtSTOMAGEN* from wheat or *Brachypodium* could effectively increase the production of stomata and clustering in *Arabidopsis* (Fig. 3G,H,K-M; Figs S2, S3). These results indicate that these *STOMAGEN*-like genes (named *STOMAGEN-1* and *STOMAGEN-2*) are orthologs of the positive stomatal EPF peptide in *Arabidopsis AtSTOMAGEN* and have been duplicated in the genomes of both grass lineages.

Grass *EPF1/EPF2* homologs complement the epidermal phenotypes of *Arabidopsis epf2* mutants

Through cross-species complementation studies, we further investigated the behavior of two *EPF1/EPF2*-like genes from wheat and *Brachypodium* in the regulation of epidermal development. We expressed each of the grass *EPF1/EPF2* homologs in *epf1* and *epf2* mutants under the control of their respective *Arabidopsis* promoters to drive their expression into distinct stages of the stomatal lineage in which *AtEPF1* and *AtEPF2* are normally expressed in *Arabidopsis*. We first confirmed that the *Arabidopsis EPF* promoters that were used for the cross-species rescue experiments drove GFP reporter activity in the corresponding stomatal precursors in the epidermis: the *AtEPF1* promoter showed expression in late meristemoids, guard mother cells (GMCs) and young guard cells; the *AtEPF2* promoter showed expression for meristemoid mother cells and early meristemoids (Fig. S4). To determine whether the grass EPF1/EPF2 peptides are functional orthologs of AtEPF1, the *Brachypodium* and wheat genes were expressed under the *AtEPF1* promoter in the *epf1* loss-of-function mutant. The *epf1* mutant exhibited the previously reported mild stomatal clustering phenotype, resulting from defects in spacing divisions (Fig. 4A,M) (Hara et al., 2007). Unlike the positive control (*AtEPF1pro::AtEPF1* in *epf1*; Fig. 4B,M), none of the genotypes expressing grass *EPF1/EPF2* homologs (*AtEPF1pro::BdEPF2-1*, *AtEPF1pro::BdEPF2-2*, *AtEPF1pro::TaEPF1* and *AtEPF1pro::TaEPF2*) was able to suppress the paired stomata phenotype of *epf1* (Fig. 4A-F,M; Fig. S5), suggesting that neither the wheat nor the *Brachypodium EPF1/EPF2*-like genes can replace the function of *AtEPF1* in *Arabidopsis*. The *EPF1/EPF2*-like genes from wheat and *Brachypodium* were then screened for complementation of the epidermal phenotypes of *epf2*, in which *epf2* displays excessive entry divisions resulting in significantly increased nonstomatal cell density (Fig. 4G,N) (Hara et al., 2009; Hunt and Gray, 2009). In this case, similar to *AtEPF2pro::AtEPF2* in *epf2* (Fig. 4H,N), expression of all grass *EPF1/EPF2* homologs driven by the endogenous *AtEPF2* promoter (*AtEPF2pro::BdEPF2-1*, *AtEPF2pro::BdEPF2-2*, *AtEPF2pro::TaEPF1* and *AtEPF2pro::TaEPF2*) significantly rescued the epidermal phenotype of the *epf2* mutant (Fig. 4G-L,N; Fig. S6). These results are congruent with the results presented above for the overexpression of *Brachypodium* or wheat *EPF1/EPF2* homologs in *Arabidopsis*. Taken together, these observations clearly indicate that either of the two most-similar AtEPF1/AtEPF2 homologs from wheat and *Brachypodium* can substitute for AtEPF2, but cannot replace the function of AtEPF1 in *Arabidopsis*.

Application of bioactive grass EPF peptides triggers stomatal developmental defects in both *Arabidopsis* and *Brachypodium* seedlings

Overexpression and cross-species complementation experiments indicated that there are two copies of stomatal EPF homologs in wheat and *Brachypodium*, each of which behaves in a similar way to AtEPF2 and AtSTOMAGEN, respectively when they are expressed in *Arabidopsis*. To determine how these grass EPF peptides regulate stomatal development in grasses, which have stomatal morphologies and patterns that differ from those of *Arabidopsis*, the epidermal phenotypic effects of *Brachypodium* seedlings (Bd21-3) treated with bioactive mature EPF peptides (MBdEPF2-1, MBdEPF2-2 and MBdSTOMAGEN-1) were examined. BdSTOMAGEN-2 was excluded from the analyses because of its relatively low level of expression in the region in developing *Brachypodium* leaves in which stomata develop, and also based on the functional redundancy with BdSTOMAGEN-1 in stomatal development when expressed in *Arabidopsis* (Fig. 2A, Fig. 3G,H,M; Fig. S2C,D). Our work focused on EPF peptides from *Brachypodium* because similar phenotypes were produced by stomatal EPF orthologs from wheat and *Brachypodium* in the experiments described above (Figs 3, 4; Figs S2-S6) and because its small size allowed for the monitoring of the epidermal phenotypes on the first leaves of seedlings by bioassays.

First, we produced C-terminal predicted mature forms of recombinant MBdEPF2-1 (91 amino acids), MBdEPF2-2 (83 amino acids) and chemically synthesized MBdSTOMAGEN-1 (45 amino acids) peptides based on the protocol we developed for *Arabidopsis* EPFs in a previous study (Fig. S7) (Lee et al., 2012). After protein refolding, we applied these bioactive grass EPF peptides to *Arabidopsis* seedlings. Application of either MBdEPF2-1

Development (2021) 148, dev199780. doi:10.1242/dev.199780

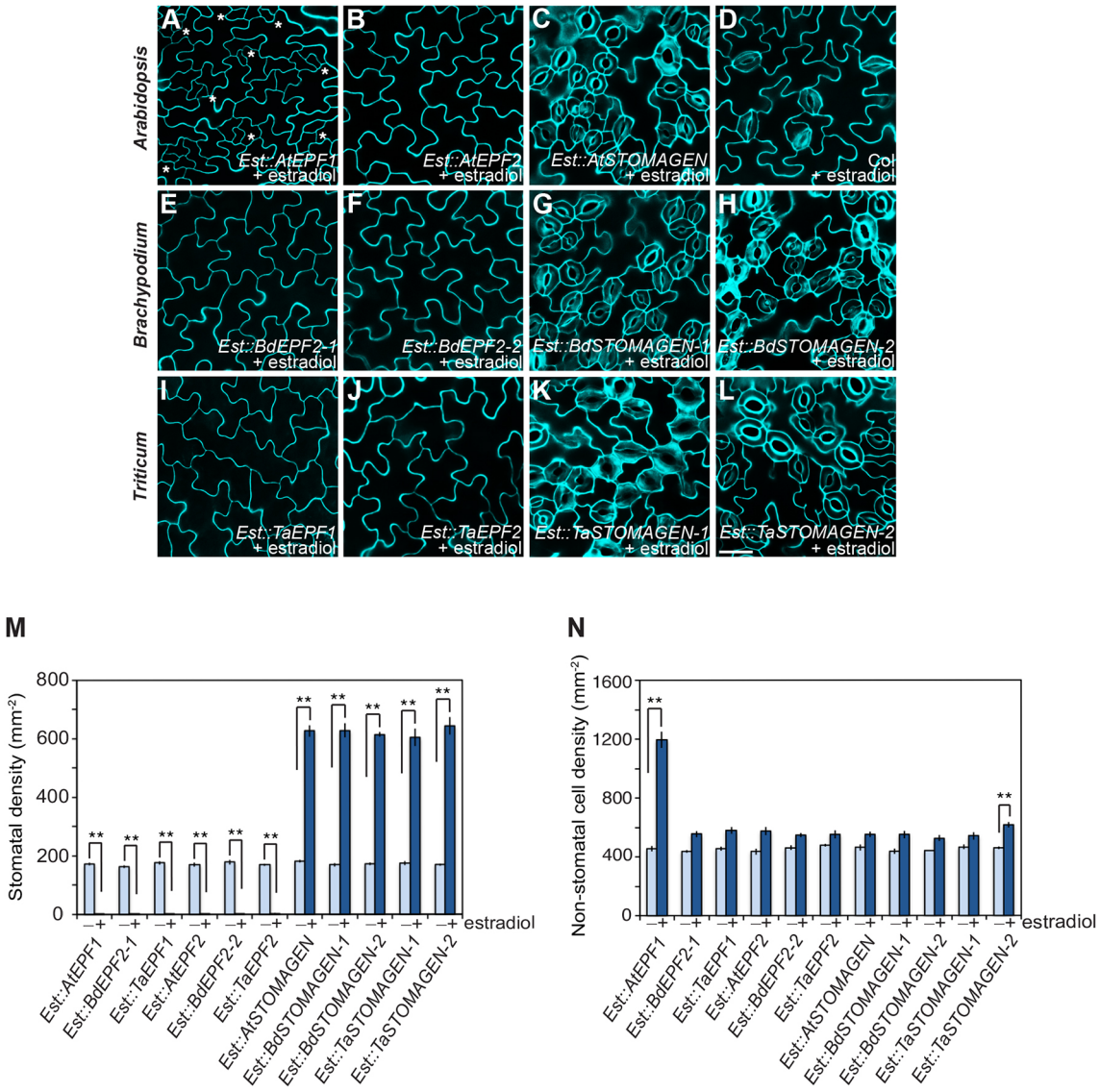

Fig. 3. Ectopic expression of grass stomatal EPF homologs exhibit stomatal development defects in *Arabidopsis*. (A-L) Representative confocal images of the abaxial cotyledon epidermis of 10-day-old *Arabidopsis* transgenic seedlings carrying estradiol-induced constructs of well-known stomatal EPF family peptides in *Arabidopsis* (A) *Est::AtEPF1*, (B) *Est::AtEPF2*, (C) *Est::AtSTOMAGEN*; stomatal EPF homologs in *Brachypodium* (E) *Est::BdEPF2-1*, (F) *Est::BdEPF2-2*, (G) *Est::BdSTOMAGEN-1* and (H) *Est::BdSTOMAGEN-2*; and wheat stomatal EPF homologs (I) *Est::TaEPF1*, (J) *Est::TaEPF2*, (K) *Est::TaSTOMAGEN-1* and (L) *Est::TaSTOMAGEN-2*. *Arabidopsis* Col wild-type seedlings in the presence of estradiol (D) and uninduced controls showed no effects on stomatal development (see Figs S2, S3). Asterisks in (A) indicate arrested stomatal precursors. Cells were outlined by propidium iodide staining (cyan), and images were taken under the same magnification. (M,N) Quantitative analysis of 10-day-old abaxial cotyledon epidermis. (M) Stomatal density (number of stomata per mm^2) and (N) nonstomatal epidermal cell density (number of nonstomatal cells per mm^2) from *Arabidopsis* transgenic seedlings harboring constructs of each of the estradiol-inducible stomatal EPF peptides in *Arabidopsis*, and their grass homologs in *Brachypodium* and wheat (dark-blue bars) compared with uninduced transgenic seedlings (light-blue bars). '–' indicates no induction and '+' indicates induced by estradiol. Overexpression of *AtEPF1*/*AtEPF2*-like genes from wheat and *Brachypodium* led to an epidermis devoid of all stomatal lineage cells, a phenotype identical to induced *Arabidopsis EPF2*, but not to *EPF1*, overexpression. By contrast, induced *STOMAGEN*-like genes in grass increased stomatal density and clustering, a phenotype identical to the *Arabidopsis STOMAGEN* overexpressor. **P<0.0001 (Student's t-test); n=8 or 9 for each genotype. The experiments were repeated three times with similar results. Data are mean±s.e.m. For a complete set of phenotypes and expression data of multiple independent transgenic plants, see Figs S2, S3. Scale bar: 30 µm.

or MBdEPF2-2 peptide rendered the *Arabidopsis* epidermis completely devoid of any stomatal lineage cells, resulting in a composition of only pavement cells, a phenotype identical to induced overexpression of *AtEPF2* (Fig. 5C,F,G) or application of recombinant AtEPF2 to *Arabidopsis* seedlings (Lee et al., 2015, 2012). By contrast, treatment of *Arabidopsis* seedlings with chemically synthesized MBdSTOMAGEN-1 promoted stomatal development and clustering, a phenotype similar to the induced *AtSTOMAGEN* overexpression (Fig. 5D,H) or treatment of bioactive AtSTOMAGEN in *Arabidopsis* (Lee et al., 2015).

Next, to investigate whether the effects of these *Brachypodium* EPF peptides observed in *Arabidopsis* would produce similar effects in *Brachypodium* itself, the leaf epidermis of MBdEPF-treated *Brachypodium* seedlings was analyzed. Given that the loss of stomata causes seedling lethality, we checked epidermal phenotypes on the first leaves of *Brachypodium* seedlings. The grass leaf

Development (2021) 148, dev199780. doi:10.1242/dev.199780

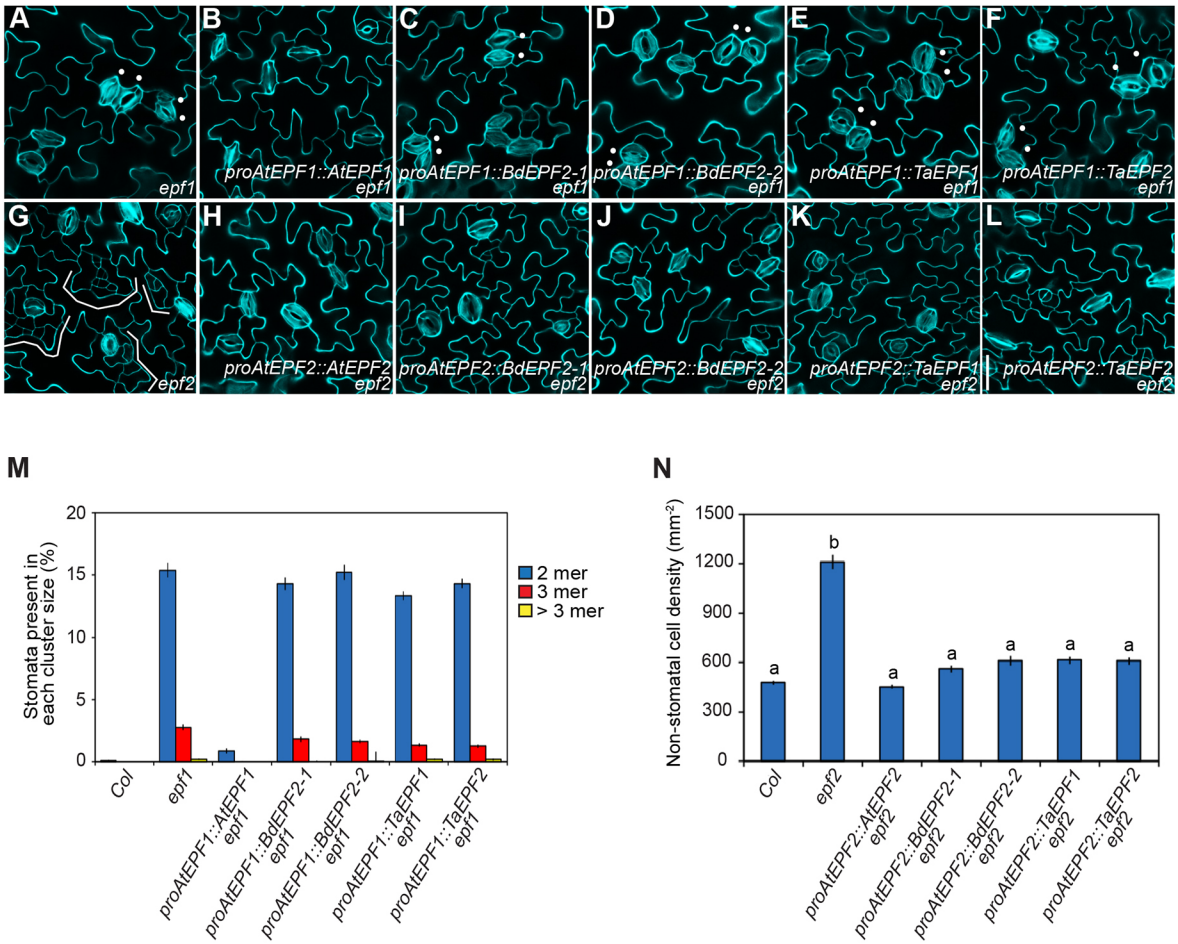

Fig. 4. Complementation of *Arabidopsis epf2* mutants by grass *EPF1*/*EPF2* homologs. (A-F) Confocal images of 10-day-old abaxial cotyledons of the (A) *Arabidopsis epf1* mutant, (B) *epf1*-expressing *proAtEPF1::AtEPF1*, (C) *proAtEPF1::BdEPF2-1*, (D) *proAtEPF1::BdEPF2-2*, (E) *proAtEPF1::TaEPF1* and (F) *proAtEPF1::TaEPF2*. Expression of *AtEPF1*, but not any of the grass *EPF1*/*EPF2*-like genes, driven by the *Arabidopsis EPF1* promoter, rescues the stomatal pairing phenotype (dots) of the *Arabidopsis epf1* mutant. (G-L) Confocal images of 10-day-old abaxial cotyledons of (G) the *Arabidopsis epf2* mutant, (H) *epf2*-expressing *proAtEPF2::AtEPF2*, (I) *proAtEPF2::BdEPF2-1*, (J) *proAtEPF2::BdEPF2-2*, (K) *proAtEPF2::TaEPF1* and (L) *proAtEPF2::TaEPF2*. Excessive entry divisions (brackets), which is the typical phenotype of the *Arabidopsis epf2* mutant, were complemented by *AtEPF2* as well as by grass *EPF1*/*EPF2*-like genes, which were expressed under the control of the *Arabidopsis EPF2* promoter. All confocal images were taken under the same magnification. (M) Percentage of stomata present in each cluster size in the *epf1* mutant and the *epf1* mutant expressing *AtEPF1* and *EPF1*/*EPF2*-like genes in *Brachypodium* and wheat. (N) Nonstomatal epidermal cell density of 10-day-old abaxial cotyledons of the *epf2* mutant and the *epf2* mutant expressing *AtEPF2* and grass *EPF1*/*EPF2* homologs. Genotypes without significantly different phenotypes are grouped together with the same letter (P<0.05, Tukey's HSD test after a one-way ANOVA). n=15–17 for each genotype. Data are mean±s.e. See also Figs S5, S6. Scale bar: 30 µm.

epidermis in the wild-type (mock-treated Bd21-3) seedlings generated orderly patterned stomata in specific cell files typically located one to two cells away from veins (arrowheads in Fig. 5I), unlike the scattered pattern of stomata in dicot *Arabidopsis* leaves. However, application of either bioactive MBdEPF2-1 or MBdEPF2-2 peptide solution resulted in the complete absence of any stomatal complexes at predictable distances from veins, whereas MBdSTOMAGEN-1 treatment promoted stomatal density and clustering in the stomatal cell files of the *Brachypodium* leaf epidermis (Fig. 5J-O, Fig. 6; Figs S9-S11). To determine the origin of stomatal defects in MBdEPF-treated *Brachypodium* seedlings, we further examined two early stages of grass stomatal development, stomatal file establishment and asymmetric division, which are found at the base of young *Brachypodium* leaves. The epidermis of Bd21-3 seedlings treated with the MBdEPF2-1 or MBdEPF2-2 peptide showed neither smaller cells nor asymmetric divisions in the stomatal cell files at the predicted distances from the veins, whereas the application of MBdSTOMAGEN-1 to Bd21-3 seedlings resulted in ectopic files with smaller cells and asymmetric divisions (Fig. S8). These results suggest that orthologs of AtEPF2 and AtSTOMAGEN may also be involved in regulating stomatal initiation in grasses, in which MBdEPF2 peptides act as inhibitors and BdSTOMAGENs act as promoters of stomatal development. However, unlike *Arabidopsis*, we also found that the application of either the MBdEPF2-1 or MBdEPF2-2 peptide failed to induce any obvious change in other nonstomatal epidermal cells, such as silica cells in veins, and hair cells, although the generation of stomata and stomatal precursors was completely blocked. The overexpression of *AtEPF2* (or application of the bioactive EPF2 peptide) in *Arabidopsis* not only blocked stomata and stomatal precursor development, but also led to development of an epidermis with only pavement cells. However, *Brachypodium* plants treated with recombinant MBdEPF2-1 or MBdEPF2-2 peptide developed hair cells instead of stomata in stomatal cell files (Fig. 5J,K,P), suggesting that the default cell fate of smaller cells of asymmetric divisions in entire epidermal lineages of grass is not affected by the

Development (2021) 148, dev199780. doi:10.1242/dev.199780

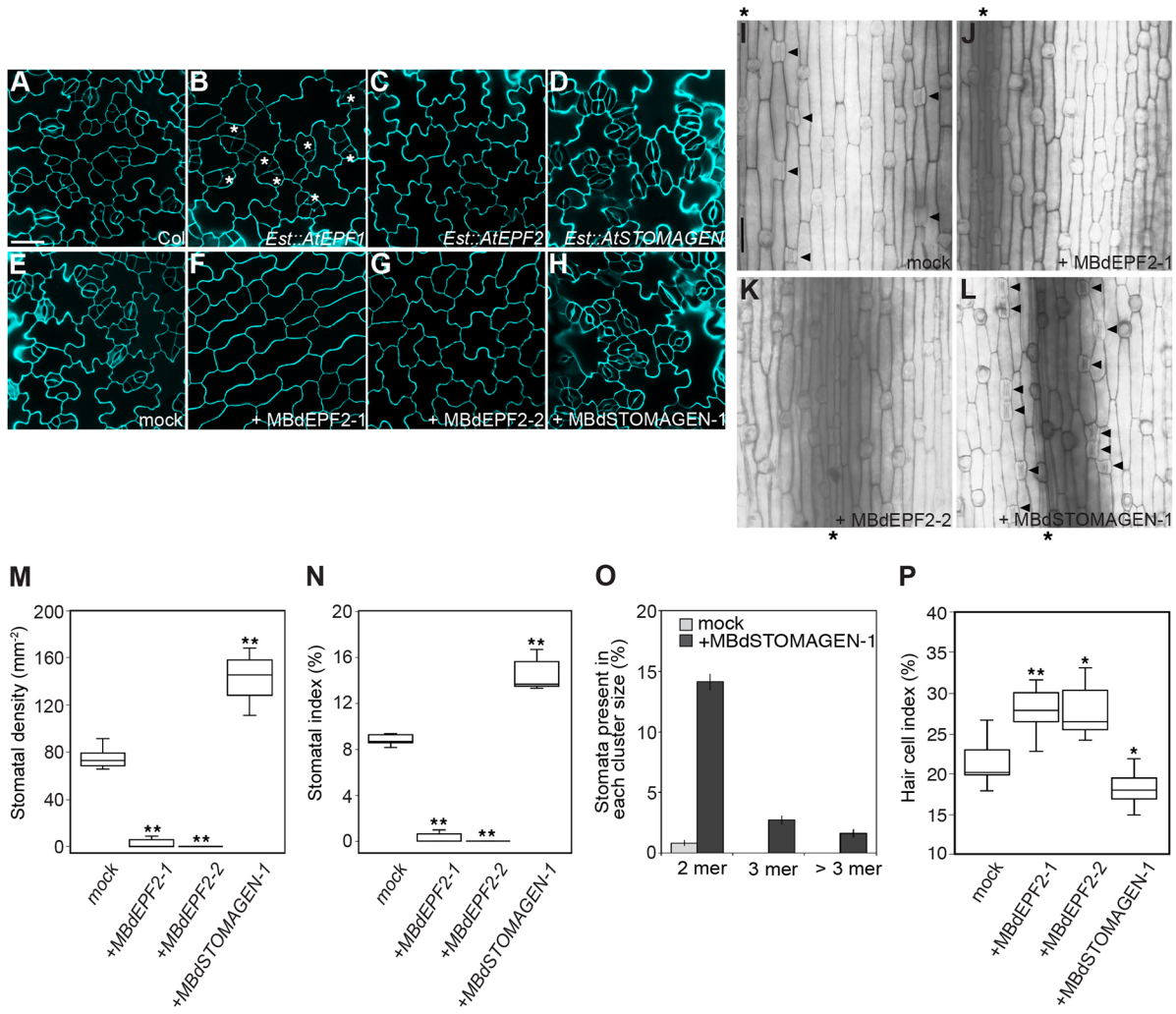

Fig. 5. Effects of the application of bioactive *Brachypodium* EPF peptides on epidermal development. (A-D) Representative confocal images of abaxial cotyledons of (A) *Arabidopsis* wild-type (Col) and (B) transgenic seedlings carrying estradiol-inducible constructs of *Arabidopsis* EPF peptides, *Est::AtEPF1*, (C) *Est::AtEPF2* and (D) *Est::AtSTOMAGEN* grown in ½ MS medium with estradiol. Asterisks in B indicate arrested stomatal precursor cells. (E-H) Abaxial epidermis of cotyledons of (E) Col seedlings grown in a buffer solution (mock), (F) 2 µM MBdEPF2-1, (G) 2 µM MBdEPF2-2 or (H) 2 µM MBdSTOMAGEN-1. Both bioactive, recombinant EPF1/EPF2-like peptides from *Brachypodium* (MBdEPF2-1 and MBdEPF2-2) inhibit stomatal lineage initiation, whereas synthetic MBdSTOMAGEN-1 peptide promotes stomatal clustering and density in *Arabidopsis*. Images were taken under the same magnification. (I-L) Optical microscopy images of abaxial epidermis of the first leaves of (I) *Brachypodium* wild-type (Bd21-3) seedlings grown in ½ MS medium with a buffer solution (mock), (J) 2 µM MBdEPF2-1, (K) 2 µM MBdEPF2-2 or (L) 2 µM MBdSTOMAGEN-1. Arrowheads indicate stomata that are always found in specific cell files adjacent to veins (marked by asterisks) in *Brachypodium*. Images were taken under the same magnification. (M-P) Quantitative analysis of abaxial leaf epidermis of Bd21-3 seedlings without (mock) or with bioactive *Brachypodium* EPF peptides (MBdEPF2-1, MBdEPF2-2 or MBdSTOMAGEN-1). (M) Stomatal density, (N) stomatal index (percentage of the number of stomata to the total number of epidermal cells), (O) stomatal cluster distribution (in %) and (P) hair cell index (percentage of the number of hair cells to the total number of epidermal cells). Application of bioactive *Brachypodium* MBdEPF2-1 or MBdEPF2-2 peptide inhibits stomatal development accompanied by default development as hair cells increased in stomatal cell files in the *Brachypodium* epidermis. By contrast, MBdSTOMAGEN-1 peptide increases stomatal density and clustering in *Brachypodium*. Peptide application experiments were performed at least five times with similar results. *n*=6-11 for each treatment. Data are mean±s.e. The median is marked as a horizontal line and upper and lower quartiles are indicated by the top and bottom of the box, respectively; whiskers indicate 1.5× the interquartile ranges. ***P*<0.001, **P*<0.01 (Student's *t*-test with data from mock-treated Bd21-3 seedlings). Scale bars: 30 µm in A; 50 µm in I.

application of these *Brachypodium* EPF peptides. By contrast, *Brachypodium* seedlings treated with MBdSTOMAGEN-1 displayed variability in the strength of the phenotype, and the seedlings showing the strongest epidermal phenotypes exhibited unusual subsidiary cell morphologies and additional ectopic stomatal cell files, in addition to increased stomatal density and stomatal patterning defects (Fig. S9A).

Given that *Brachypodium* leaves produce highly spatially and temporally organized stomatal development from the base to the tip, we next examined potential roles of BdSTOMAGEN-1 in later stages of grass stomatal development by observing cells at the subsidiary cell formation and GMC division stages. Application of MBdSTOMAGEN-1 to *Brachypodium* seedlings resulted in abnormal subsidiary cell formation by spanning multiple smaller daughter cells, by becoming stomatal precursors (GMCs) or by producing extra irregular asymmetric divisions in the cells neighboring the GMCs (Fig. S9B). This indicates that BdSTOMAGEN-1 may have an additional role in promoting asymmetric divisions to produce both stomatal precursors and subsidiary cells, in addition to initiating stomatal cell files during grass stomatal development. In summary, our data indicate that *Brachypodium* EPF peptides BdEPF2s and BdSTOMAGENs are

Development (2021) 148, dev199780. doi:10.1242/dev.199780

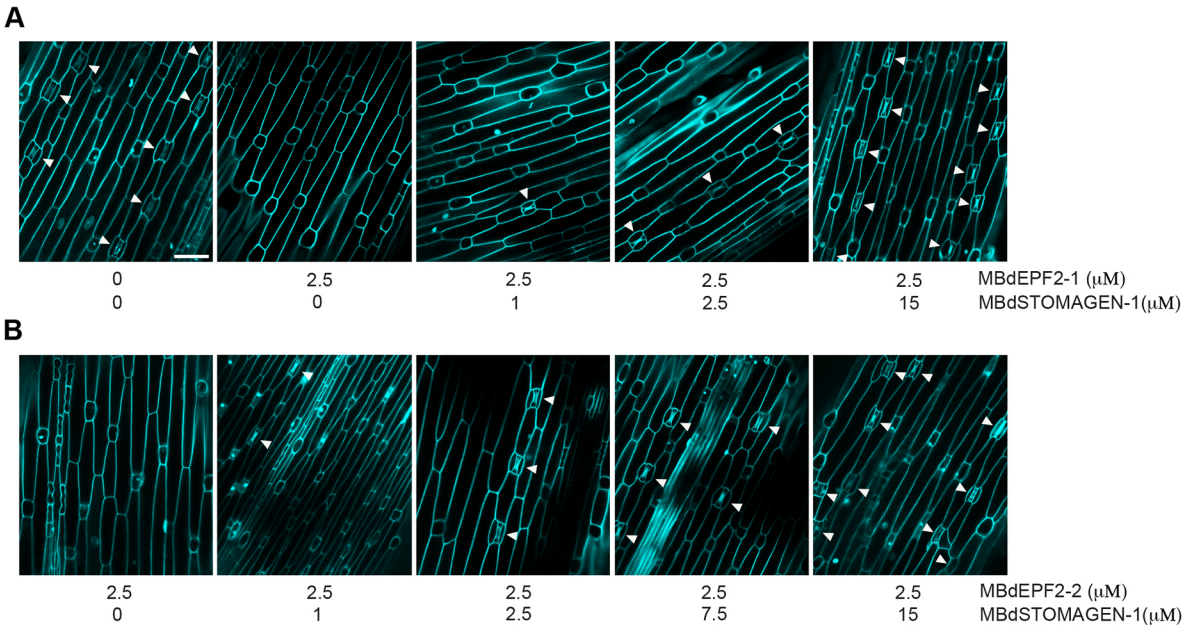

Fig. 6. BdEPF2 activity is antagonized by that of BdSTOMAGEN-1 in *Brachypodium*. (A) *Brachypodium* wild-type (Bd21-3) seedlings treated with a buffer solution, MBdEPF2-1 alone, or mixtures containing MBdEPF2-1 and increasing concentrations of MBdSTOMAGEN-1. (B) *Brachypodium* Bd21-3 seedlings treated with MBdEPF2-2 alone, or mixtures containing MBdEPF2-2 plus increasing concentrations of MBdSTOMAGEN-1. Biological activity of MBdEPF2 peptides inhibiting grass stomatal development was suppressed by MBdSTOMAGEN-1. Arrowheads indicate stomata that are always found in specific cell files adjacent to veins in *Brachypodium* leaves. Images were taken under the same magnification. See also Fig. S10 for contrasting results using another EPF-family member in *Brachypodium*, MBd2g53661, and Fig. S11 for the effect of MBdEPF2-2 in the presence of MBdSTOMAGEN-1. Scale bar: 50 µm.

key secreted signaling peptides with opposing functions in controlling stomatal initiation in *Brachypodium*. Unlike BdEPF2s, which specifically control the early step of grass stomatal development (the establishment of stomatal cell files), our results also suggest that BdSTOMAGEN regulates several stages of stomatal development and patterning in grasses.

Duplicated grass EPF peptides, BdEPF2 and BdSTOMAGEN, compete for grass stomatal development

Given that both BdEPF2-1 and BdEPF2-2 inhibit grass stomatal initiation whereas BdSTOMAGENs act as stomata-inducing signals, we next examined whether biological activity of these BdEPF2 peptides is inhibited by the contrasting BdSTOMAGEN peptide. Application of either MBdEPF2-1 or MBdEPF2-2 peptide to *Brachypodium* wild-type seedlings inhibited stomatal development as described above, but by co-incubating with increasing concentrations of BdSTOMAGEN-1 peptide, the stomataless phenotype was restored to a nearly normal epidermis with stomata in a dose-dependent manner (Fig. 6). To ensure the specificity of these results, we also refolded chemically synthesized MBd2g53661 peptide, another member of the EPF family in *Brachypodium*, which our expression analysis indicated is expressed in young leaves in which stomata develop (Fig. 2A; Fig. S7). Exposure of both *Arabidopsis* and *Brachypodium* seedlings to MBd2g53661 peptide solution demonstrated that the Bd2g53661 peptide does not have a role in stomatal development (Fig. S10), unlike the grass EPF peptides we have investigated. Exposure of Bd21-3 seedlings to mixtures of bioactive MBdEPF2-2 plus higher concentrations of MBd2g53661 peptide did not affect the capacity of MBdEPF2 to inhibit stomatal development in *Brachypodium* (Fig. S10B). This clearly indicates that the effects of the positive regulator MBdSTOMAGEN on two MBdEPF2-treated stomataless *Brachypodium* epidermises are the result of their specific antagonistic behaviors in controlling grass stomatal development. Given that BdSTOMAGEN-1-treated *Brachypodium* seedlings often develop stomata with unusual subsidiary cell morphologies (Fig. S9), we also investigated the effect of MBdEPF2-2 on the subsidiary cell defects found on MBdSTOMAGEN-1-treated *Brachypodium* epidermises. The stomata-inducing phenotype of the MBdSTOMAGEN-1 application was suppressed by MBdEPF2-2, but the subsidiary cell defect phenotype of MBdSTOAGEN-1-treated seedlings was unaffected (Fig. S11). This result further emphasizes that the antagonistic relationship of BdEPF2 and BdSTOMAGEN is specific to the early stage of stomatal development in *Brachypodium*.

DISCUSSION

The present study aimed to identify EPF peptides and their biological functions in grasses because this group of plants includes several of the most important agricultural crops, and because grasses generally have different developmental processes compared with dicots. We found that all major cereal plants examined have genes encoding 11-15 putative EPF peptides, including at least two homologs of *AtEPF1* and *AtEPF2* and two *AtSTOMAGEN*-like genes, suggesting that the EPF family of secreted cysteine-rich peptides are signaling molecules conserved between dicots and grasses. Our work also revealed that four grass EPF peptides, which are homologs to known stomatal *Arabidopsis* EPFs, are duplicated grass orthologs of AtEPF2 and AtSTOMAGEN, and that these two classes of signalling peptide have opposing activity in controlling the early stage of stomatal development, stomatal cell file establishment, in grasses.

In *Arabidopsis*, although two negative stomatal signals, AtEPF1 and AtEPF2, have strong sequence similarity, these EPF peptides control two distinct steps of stomatal development: AtEPF1 inhibits

Development (2021) 148, dev199780. doi:10.1242/dev.199780

stomatal differentiation and enforces spacing division, and AtEPF2 inhibits initiation of the stomatal cell lineage (Hara et al., 2007, 2009; Hunt and Gray, 2009). Recent studies of *AtEPF1/AtEPF2*-like and *STOMAGEN*-like genes in some grass species indicate that they have a role in controlling stomatal differentiation (Caine et al., 2019; Dunn et al., 2019; Hughes et al., 2017; Lu et al., 2019; Yin et al., 2017). For example, although overexpression of one of the *AtEPF1/AtEPF2*-related genes in barley (*Hordeum vulgare*), *HvEPF1*, decreased stomatal density, it also significantly increased nonstomatal cells by increasing the density of arrested stomatal precursors, similar to the *Arabidopsis EPF1* overexpressor (Hughes et al., 2017). By contrast, our functional analyses of two *AtEPF1/AtEPF2*-like genes found in wheat (*TaEPF1* and *TaEPF2*) and *Brachypodium* (*BdEPF2-1* and *BdEPF2-2*) demonstrated that they all play an important role in regulating stomatal initiation rather than stomatal differentiation or progression, which indicates that *AtEPF1/AtEPF2*-like genes in these two species behave in a similar way to *Arabidopsis EPF2* (Figs 3, 4, Figs S2-S6). Our conclusion concerning the function of the two grass EPF1/EPF2-like peptides examined was further supported by bioassays with the predicted mature *Brachypodium* EPF (MBdEPF) peptides. Similar to *AtEPF2* overexpression (or application of mature AtEPF2 peptide), the application of either of the bioactive, recombinant EPF1/EPF2-like peptides from *Brachypodium*, MBdEPF2-1 and MBdEPF2-2, led to an epidermis completely devoid of any stomatal precursors and stomata in both *Arabidopsis* and *Brachypodium*, a result that is similar to the overexpression of *AtEPF2* in *Arabidopsis* or to treatment with the mature AtEPF2 peptide (Figs 5, 6; Fig. S8). By contrast, another EPF peptide homolog in *Brachypodium*, MBd2g53661, was found to not affect stomatal development (Fig. S10). Thus, consistent with our overexpression and cross-species complementation studies, these results clearly indicate the specific roles for BdEPF2-1 and BdEPF2-2 in inhibiting entry into the stomatal lineage during stomatal development in both *Arabidopsis* and *Brachypodium*. Our findings demonstrate how various grass species use conserved EPF peptides differently to control stomatal development, which highlights the importance of examining multiple species to understand fully the function of each EPF family member in grass stomatal development.

The difference in observations for the effects of TaEPF1 and TaEPF2 reported here, and those reported in barley for HvEPF1 (Hughes et al., 2017), are surprising given that *T. aestivum* and *H. vulgare* are phylogenetically very closely related, and the active peptides for the two species differ by only two amino acids out of 52; by contrast, TaEPF1 and TaEPF2 are only 78% similar. While this paper was in preparation, Dunn et al. (2019) reported that overexpression of *EPF1/EPF2*-like genes from *T. aestivum* led to slight stomatal reduction with increased nonstomatal cell density. There are subtle differences in the experimental methods used in these studies that may contribute to these differences. Given that the loss of stomata is typically lethal, we used a chemically inducible gene expression technique that allowed quantitative induction of transgene expression, enabling some circumnavigation around the lethal effects of overexpressing key stomatal regulators. Both the two EPF1/EPF2-like peptides from *Brachypodium*, and those from wheat, inhibited stomatal development in transgenic *Arabidopsis* as effectively as the native *Arabidopsis* EPF2, a result that was also clearly observed with the treatment of plants with recombinant MBdEPF2 peptides (Figs 3, 5). By contrast, Hughes et al. (2017) and Dunn et al. (2019) used transgenic plants with constitutive overexpression, and reported that overexpression of *HvEPF1* (and *TaEPF1* or *TaEPF2*) was not able to reduce stomatal density by as much compared with *Arabidopsis* EPF1 or EPF2. It is possible that the different phenotypes observed did not include the strongest phenotypic classes (those completely lacking stomata produced by overexpression of *HvEPF1*) given that such plants may not have survived, and the plants that were characterized had low-to-moderate levels of transgene expression (Dunn et al., 2019; Hughes et al., 2017). Other subtle differences in experimental methods, such as dosage and timing of the treatment, may also contribute to these differences, and future studies of the spatial and temporal expression of EPF peptides in each grass species may help our understanding of how each grass EPF controls stomatal patterning and the major stages of grass stomatal development. As mentioned above, the application of recombinant MBdEPF2 peptides to *Brachypodium* inhibited the development of stomata within stomatal cell files but did not influence any other epidermal cell types, such as hair cells. This specific behavior found in *Brachypodium* seedlings might be attributed to grass-specific stomatal development patterns, which have evolved different roles for EPF1 and EPF2 in *Arabidopsis* that are not observed for grasses, exemplified here by wheat and *Brachypodium*.

The functions of grass EPF gene family members other than the four EPF homologs of *Arabidopsis* stomatal peptides AtEPF1, AtEPF2, and AtSTOMAGEN that we have investigated, remain unknown. Considering that some grass EPF family members, such as *Bd3g58660* and *Ta2g317000*, are highly expressed in young leaves in which stomata develop in *Brachypodium* and wheat (Fig. 2A,B), it is possible that other grass EPF family members, which we identified by phylogenetic analyses, serve as ligands to control different stages of grass stomatal development, such as asymmetric division to create stomatal precursors or their grass-specific adjacent subsidiary cells and stomatal differentiation. Thus, future investigation of the remaining grass EPF homologs would provide comprehensive insight into the role of EPF peptide signaling in grass developmental processes, including stomatal patterning.

Although the EPF1, EPF2 and STOMAGEN peptides have been shown to interact with TMM and ERECTA family receptor kinases, none of the work with grass homologs of *Arabidopsis* stomatal receptors has yet demonstrated the roles of orthologous receptors in grass stomatal development. The existence of antagonist regulation of grass stomatal development by duplicated orthologs of *Arabidopsis* AtEPF2 and AtSTOMAGEN suggests that stomatal initiation in both plant species may be regulated by naturally occurring agonistic and antagonistic ligands for the same receptor, despite differences in their stomatal patterns. Application of either the MBdEPF2-1 or MBdEPF2-2 peptide to *Brachypodium* wild-type seedlings inhibited stomatal development, whereas its co-incubation with increasing concentrations of MBdSTOMAGEN-1 resulted in a nearly normal stomatal density without increased stomatal clustering even when *Brachypodium* seedlings were treated with very high concentrations of MBdSTOMAGEN-1 compared with the MBdEPF2 peptide (Fig. 6; Fig. S9). Thus, unlike *Arabidopsis*, in which AtSTOMAGEN and AtEPF2 peptides directly compete for the ERECTA receptor kinase, it is possible that positive and negative stomatal EPF peptides in grasses either have different target receptors, thereby influencing each other's signaling indirectly, or may bind to the same receptor but with a different binding affinity.

Besides regulating the entry into the stomatal lineage, we found that BdSTOMAGENs may regulate many aspects of stomatal development (i.e. subsidiary cell formation) in *Brachypodium*. In rice, loss of one of the *STOMAGEN*-like genes, *OsEPFL9-1*, results

Development (2021) 148, dev199780. doi:10.1242/dev.199780

in reduced stomatal formation, whereas overexpression of another rice *STOMAGEN*-like gene, *OsEPFL9-2*, in *Arabidopsis* showed mild hypocotyl-specific stomatal patterning defects, suggesting their divergent roles in rice stomatal development (Lu et al., 2019; Yin et al., 2017). These differences indicate that, although different grass species use homologs of well-known stomatal AtEPFs, they may regulate their stomatal development in a species-specific manner. Future investigations of the linkage of grass STOMAGENs to distinct stages of grass stomatal development or to a specific organ, by expressing BdSTOMAGEN under the control of each organ-specific or grass stomatal lineage cell type promoter, will provide insight into how BdSTOMAGENs function in a specific phase or organ of grass stomatal development. The work presented herein shows that the regulation of stomatal development by secreted EPF peptides is, to a great extent, conserved in two major classes of flowering plant, and creates significant potential for the agricultural use of peptide treatments to improve crop productivity and water-use efficiency.

MATERIALS AND METHODS

Plant materials and growth conditions

The *Arabidopsis* ecotype Columbia (Col) was used as a wild-type control in the *Arabidopsis* study. The following mutants and transgenic plants were described previously: *epf1* (Hara et al., 2007), *epf2* (Hara et al., 2009), *proEst::AtEPF1* and *proEst::AtEPF2* (Lee et al., 2012), and *proEst::AtSTOMAGEN* (Lee et al., 2015). Each transgene was introduced into Col and the respective mutant backgrounds by *Agrobacterium*-mediated transformation. The wheat (*T. aestivum L.*) genotype Chinese Spring was used for isolation of gene sequences and expression analysis. *Brachypodium* line Bd21-3 was used for isolation of gene sequences, expression studies and peptide bioassays. Seeds were surface sterilized with bleach solution [with 3.4% sodium hypochlorite (diluted from 10.3% bleach) and 0.01% Triton-X 100] and plated on ½ Murashige–Skoog (MS) agar plates (Caisson Labs). When needed, 5- to 6-day-old *Brachypodium* and wheat seedlings and 10-day-old *Arabidopsis* seedlings were transferred to soil and grown at 22°C under long-day conditions (18 h light/6 h dark).

Phylogenetic analysis

The amino acid sequences of the known or predicted mature EPF peptides previously identified in *Arabidopsis* and rice (Takata et al., 2013) were used as query sequences to identify homologous gene sequences for *T. aestivum* in the Transcriptome Shotgun Assembly (TSA) databases of the National Center for Biological Information (NCBI) by tBlastn. The TSA contigs were used to search the NCBI EST database and the International Wheat Genome Sequencing Consortium (IWGSC) (International Wheat Genome Sequencing, 2014) of wheat survey sequences (WSS) of individual chromosome arms, versions 2 and 3. The sequences were also reconfirmed, and assigned to specific wheat chromosomes using the IWGSC whole-genome assembly RefSeq v1.0 (Alaux et al., 2018; International Wheat Genome Sequencing, 2014; International Wheat Genome Sequencing et al., 2018). Comparison to the sequences of the whole-genome assembly was used to identify homeologous copies of the gene family members from the A, B and D genomes of *T. aestivum*. Novel sequences identified in genomic databases were used iteratively to query the TSA and EST databases to verify the sequences and to identify correctly the exon/intron junctions in the genomic sequences. In cases in which there was discrepancy between sequences from different databases, contigs of the transcripts were reassembled with *T. aestivum* EST sequences that shared a minimum of 99% identity, using the CAP3 assembly program at PRABI (Huang and Madan, 1999). Gene identifiers for *T. aestivum* used in the study were from the Ensembl Plant database (http://plants.ensembl.org/) and those for *Brachypodium* were from the Phytozome 12 database (https://phytozome.jgi.doe.gov/). EPF gene family members identified in *T. aestivum* were used to identify homologs in other monocotyledonous species. Sequences for EPF genes in other species were taken from the following databases: *S. bicolor*, PlantGDB (http://www.plantgdb.org/SbGDB/); *O. sativa*, Rice Annotation Project Database (https://rapdb.dna.affrc.go.jp/); *Zea mays*, GenBank, (https://www.ncbi.nlm.nih.gov/); *B. distachyon*, Phytozome v12 (https://phytozome.jgi.doe.gov/); *H. vulgare*, IPK (http://webblast.ipk-gatersleben.de/); and *A. thaliana*, UniProt (https://www.uniprot.org/uniprot/). An initial phylogenetic tree for the heuristic search was obtained automatically by applying neighbor-joining and BioNJ algorithms to a matrix of pairwise distances estimated using a Jones Taylor Thornton (JTT) model and then selecting the topology with superior log likelihood value. The analysis involved 87 amino acid sequences. All positions with less than 95% site coverage were eliminated; that is, fewer than 5% alignment gaps, missing data and ambiguous bases were allowed at any position. These procedures were performed using MEGA software (version 7.0) (Kumar et al., 2016). Tables S1 and S2 list the amino acid sequences of grass EPF peptides used.

Plasmid construction and generation of transgenic plants

The following constructs were generated and used in this study: pJSL156 (*BdEPF2-1* cDNA); pJSL151 (*proEst::BdEPF2-1*); pJSL157 (*BdEPF2-2* cDNA); pJSL158 (*proEst::BdEPF2-2*); pJSL148 (*BdSTOMAGEN-1* cDNA); pJSL149 (*proEst::BdSTOMAGEN-1*); pJSL185 (*BdSTOMAGEN-2* cDNA); pJSL187 (*proEst::BdSTOMAGEN-2*); pJSL171 (*TaEPF1* cDNA); pJSL179 (*proEst::TaEPF1*); pJSL173 (*TaEPF2* cDNA); pJSL180 (*proEst::TaEPF2*); pJSL177 (*TaSTOMAGEN-1* cDNA); pJSL181 (*proEst::TaSTOMAGEN-1*); pJSL188 (*proEst::TaSTOMAGEN-2*); pJSL193 (*AtEPF1* cDNA); pRJ14 (*proAtEPF1::nucGFP*); pRJ21 (*proAtEPF1::AtEPF1*); pRJ6 (*proAtEPF1::BdEPF2-1*); pRJ13 (*proAtEPF1::BdEPF2-2*); pRJ9 (*proAtEPF1::TaEPF1*); pRJ18 (*proAtEPF1::TaEPF2*); pJSL146 (*AtEPF2* promoter); pJSL194 (*AtEPF2* cDNA); pRJ23 (*proAtEPF2::nucGFP*); pRJ22 (*proAtEPF2::AtEPF2*); pJSL175 and pRJ17 (*proAtEPF2::BdEPF2-1*); pRJ16 (*proAtEPF2::BdEPF2-2*); pJSL190 and pRJ20 (*proAtEPF2::TaEPF1*); pRJ19 (*proAtEPF2::TaEPF2*); pJSL198 (*pBAD::MBdEPF2-1-6xHis*); and pJSL199 (*pBAD::MBdEPF2-2-6xHis*). Plasmid pER8 (Zuo et al., 2000) was used for estradiol-inducible constructs, and the Gateway-cloning system (Invitrogen) was used to generate most constructs for the cross-species complementation studies. Tables S4 and S5 detail the plasmid constructions and primers used. Stable transgenic *Arabidopsis* plants were generated using *Agrobacterium*-mediated transformation by the floral dipping method (Clough and Bent, 1998). More than 30 independent transgenic T1 or T2 lines per construct were screened and subjected to detailed phenotypic characterization.

RNA extraction and quantitative real-time qPCR analysis

Total RNA from different plant tissues of *Brachypodium*, wheat, and 10-day-old *Arabidopsis* transgenic seedlings grown on ½ MS plates with or without 30 µM estradiol were isolated using the RNeasy Plant Mini Kit (Qiagen) and treated with DNaseI (Qiagen) according to the manufacturer's instructions. The first-strand cDNA was generated by iScript cDNA Synthesis kit (Bio-Rad) using 1.2 µg of RNA (except for wheat, for which 100 ng of RNA was used), diluted 1:10 in double-distilled water and then used as a template for qPCR analysis. RT-qPCR analysis was performed using a CFX96 real-time PCR detection system (Bio-Rad) using SsoAdvanced Universal SYBR Green Supermix (Bio-Rad) and standard qPCR conditions in at least three technical and three biological replicates. Data were normalized against *eIF4A*, *BdUBC18* (Hong et al., 2008) and *TaRP15* (Shaw et al., 2012) for genes in *Arabidopsis*, *Brachypodium* and wheat, respectively. The Pfaffl method (Pfaffl, 2001) was used to calculate the relative expression levels of the target genes. The gene-specific primers used to detect transcripts are listed in Table S5.

Microscopy and quantitative analysis of stomatal phenotype

Confocal images were taken using a Nikon C2 operated by NIS-Elements to capture propidium iodide staining (2mg ml^{-1}; Sigma-Aldrich) to visualize cell outlines and GFP fluorescences as previously described (Tamnanloo et al., 2018). All image processing was performed using Fiji software, and the images were false colored using Photoshop CS6 (Adobe). For quantitative analysis, the central area of abaxial cotyledons of 10-day-old

Arabidopsis seedlings and the base of the first leaves of 6- to 8-day-old *Brachypodium* seedlings were stained with Toluidine Blue O (TBO) (Sigma) as previously reported (Hara et al., 2009), and images were taken using a Nikon Eclipse TiE microscope equipped with a DsRi2 digital camera (Nikon). The number of stomata and other epidermal cells in each photograph were counted and converted into both density and index measurements for each cell type. The statistically significant differences in a panel of different genotypes were determined by either a Tukey's HSD test after a one-way ANOVA ($P<0.05$) or a Student's *t*-test with *P* values of **<0.001 or *<0.01.

Chemical treatments

Transgenic *Arabidopsis* seedlings carrying estradiol-inducible EPF and *Brachypodium* and wheat homolog constructs were germinated on ½ MS medium in the absence or presence of 30 µM estradiol (Sigma) or 1-day-old transgenic seedlings grown in ½ MS medium were treated with or without 10 µM estradiol. The induction of EPF gene expression was confirmed by RT-qPCR analysis. The phenotypic consequence of induction was examined by observing the epidermal phenotype of cotyledons using a Nikon C2 laser scanning confocal microscope.

Production of peptides and bioassays

Expression and purification of *Brachypodium* MBdEPF2-1 and MBdEPF2-2 peptides were performed as described previously (Lee et al., 2012). These two recombinant peptides and chemically synthesized *Brachypodium* MBdSTOMAGEN-1 and MBd2g53661 (Invitrogen) were dissolved in 20 mM Tris-HCl, pH 8.8, and 50 mM NaCl and refolded (using a Mini Dialysis Kit, MWCO:1000, GE Healthcare) for 3 days at 4°C using glutathione (reduced and oxidized forms; Sigma) and L-arginine ethyl ester dihydrochloride (Sigma). The peptides were further dialyzed twice against 50 mM Tris-HCl, pH 8.0 for 1.5 days to remove glutathione. For bioassays, either a buffer solution alone (mock: 50 mM Tris-HCl at pH 8.0) or *Brachypodium* EPF peptides (2.5 µM) in buffer solution were applied to 1-day-old Col and Bd21-3 seedlings in ½ MS medium. After 6-8 days of further incubation, the epidermal phenotypes of abaxial *Arabidopsis* cotyledons and *Brachypodium* leaves were examined with a Nikon C2 confocal microscope and/or a Nikon Eclipse TiE microscope after TBO staining.

Acknowledgements

We thank Dr Keiko Torii (University of Texas, USA) for sharing seeds and plasmids with us, and we thank Sahar Soodbakhsh (McGill University, Canada) for plant care.

Competing interests

The authors declare no competing or financial interests.

Author contributions

Conceptualization: N.A.F., J.S.L.; Methodology: R.J.; Validation: R.J., S.C.B., P.K., P.J.G., J.S.L.; Formal analysis: R.J., S.C.B., P.J.G., J.S.L.; Investigation: R.J., S.C.B., X.W., P.K., J.S.L.; Resources: R.J., X.W., J.S.L.; Writing - original draft: P.J.G., J.S.L.; Writing - review & editing: R.J., S.C.B., P.J.G., N.A.F., S.W., J.S.L.; Visualization: R.J., S.C.B., P.J.G., J.S.L.; Supervision: P.J.G., S.W., J.S.L.; Project administration: R.J., J.S.L.; Funding acquisition: N.A.F., J.S.L.

Funding

This work was supported by funding from the Natural Sciences and Engineering Research Council of Canada (NSERC) Discovery program to J.S.L. and Alberta Innovates Bio Solutions and Alberta Wheat Commission to J.S.L. and N.A.F. X.W. was supported by the China Scholarship Council. J.S.L. was a Concordia University Research Chair.

Peer review history

The peer review history is available online at https://journals.biologists.com/dev/article-lookup/doi/10.1242/dev.199780

References

Alaux, M., Rogers, J., Letellier, T., Flores, R., Alfama, F., Pommier, C., Mohellibi, N., Durand, S., Kimmel, E., Michotey, C. et al. (2018). Linking the International Wheat Genome Sequencing Consortium bread wheat reference genome sequence to wheat genetic and phenomic data. *Genome Biol.* **19**, 111. doi:10.1186/s13059-018-1491-4

Cai, S., Papanatsiou, M., Blatt, M. R. and Chen, Z. H. (2017). Speedy grass stomata: emerging molecular and evolutionary features. *Mol Plant* **10**, 912-914. doi:10.1016/j.molp.2017.06.002

Caine, R. S., Yin, X., Sloan, J., Harrison, E. L., Mohammed, U., Fulton, T., Biswal, A. K., Dionora, J., Chater, C. C., Coe, R. A. et al. (2019). Rice with reduced stomatal density conserves water and has improved drought tolerance under future climate conditions. *New Phytol.* **221**, 371-384. doi:10.1111/nph.15344

Chen, Z. H., Chen, G., Dai, F., Wang, Y., Hills, A., Ruan, Y. L., Zhang, G., Franks, P. J., Nevo, E. and Blatt, M. R. (2017). Molecular evolution of grass stomata. *Trends Plant Sci.* **22**, 124-139. doi:10.1016/j.tplants.2016.09.005

Clough, S. J. and Bent, A. F. (1998). Floral dip: a simplified method for Agrobacterium-mediated transformation of Arabidopsis thaliana. *Plant J.* **16**, 735-743. doi:10.1046/j.1365-313x.1998.00343.x

Dunn, J., Hunt, L., Afsharinafar, M., Meselmani, M. A., Mitchell, A., Howells, R., Wallington, E., Fleming, A. J. and Gray, J. E. (2019). Reduced stomatal density in bread wheat leads to increased water-use efficiency. *J. Exp. Bot.* **70**, 4737-4748. doi:10.1093/jxb/erz248

Hara, K., Kajita, R., Torii, K. U., Bergmann, D. C. and Kakimoto, T. (2007). The secretory peptide gene EPF1 enforces the stomatal one-cell-spacing rule. *Genes Dev.* **21**, 1720-1725. doi:10.1101/gad.1550707

Hara, K., Yokoo, T., Kajita, R., Onishi, T., Yahata, S., Peterson, K. M., Torii, K. U. and Kakimoto, T. (2009). Epidermal cell density is autoregulated via a secretory peptide, EPIDERMAL PATTERNING FACTOR 2 in Arabidopsis leaves. *Plant Cell Physiol.* **50**, 1019-1031. doi:10.1093/pcp/pcp068

Hepworth, C., Caine, R. S., Harrison, E. L., Sloan, J. and Gray, J. E. (2018). Stomatal development: focusing on the grasses. *Curr. Opin. Plant Biol.* **41**, 1-7. doi:10.1016/j.pbi.2017.07.009

Hetherington, A. M. and Woodward, F. I. (2003). The role of stomata in sensing and driving environmental change. *Nature* **424**, 901-908. doi:10.1038/nature01843

Hong, S. Y., Seo, P. J., Yang, M. S., Xiang, F. and Park, C. M. (2008). Exploring valid reference genes for gene expression studies in Brachypodium distachyon by real-time PCR. *BMC Plant Biol.* **8**, 112. doi:10.1186/1471-2229-8-112

Huang, X. and Madan, A. (1999). CAP3: A DNA sequence assembly program. *Genome Res.* **9**, 868-877. doi:10.1101/gr.9.9.868

Hughes, J., Hepworth, C., Dutton, C., Dunn, J. A., Hunt, L., Stephens, J., Waugh, R., Cameron, D. D. and Gray, J. E. (2017). Reducing stomatal density in barley improves drought tolerance without impacting on yield. *Plant Physiol.* **174**, 776-787. doi:10.1104/pp.16.01844

Hunt, L., Bailey, K. J. and Gray, J. E. (2010). The signalling peptide EPFL9 is a positive regulator of stomatal development. *New Phytol.* **186**, 609-614. doi:10.1111/j.1469-8137.2010.03200.x

Hunt, L. and Gray, J. E. (2009). The signaling peptide EPF2 controls asymmetric cell divisions during stomatal development. *Curr. Biol.* **19**, 864-869. doi:10.1016/j.cub.2009.03.069

International Wheat Genome Sequencing Consortium (IWGSC) (2014). A chromosome-based draft sequence of the hexaploid bread wheat (Triticum aestivum) genome. *Science* **345**, 1251788. doi:10.1126/science.1251788

International Wheat Genome Sequencing Consortium (IWGSC), IWGSC RefSeq principal investigators, Appels, R., Eversole, K., Feuillet, C., Keller, B., Rogers, J., Stein, N., IWGSC whole-genome assembly principal investigators, Pozniak, C. J. et al. (2018). Shifting the limits in wheat research and breeding using a fully annotated reference genome. *Science* **361**, eaar7191.

Kondo, T., Kajita, R., Miyazaki, A., Hokoyama, M., Nakamura-Miura, T., Mizuno, S., Masuda, Y., Irie, K., Tanaka, Y., Takada, S. et al. (2010). Stomatal density is controlled by a mesophyll-derived signaling molecule. *Plant Cell Physiol.* **51**, 1-8. doi:10.1093/pcp/pcp180

Kosentka, P. Z., Overholt, A., Maradiaga, R., Mitoubsi, O. and Shpak, E. D. (2019). EPFL signals in the boundary region of the SAM restrict its size and promote leaf initiation. *Plant Physiol.* **179**, 265-279. doi:10.1104/pp.18.00714

Kumar, S., Stecher, G. and Tamura, K. (2016). MEGA7: molecular evolutionary genetics analysis version 7.0 for bigger datasets. *Mol. Biol. Evol.* **33**, 1870-1874. doi:10.1093/molbev/msw054

Lawson, T. and Blatt, M. R. (2014). Stomatal size, speed, and responsiveness impact on photosynthesis and water use efficiency. *Plant Physiol.* **164**, 1556-1570. doi:10.1104/pp.114.237107

Lee, J. S., Hnilova, M., Maes, M., Lin, Y. C., Putarjunan, A., Han, S. K., Avila, J. and Torii, K. U. (2015). Competitive binding of antagonistic peptides fine-tunes stomatal patterning. *Nature* **522**, 439-443. doi:10.1038/nature14561

Lee, J. S., Kuroha, T., Hnilova, M., Khatayevich, D., Kanaoka, M. M., McAbee, J. M., Sarikaya, M., Tamerler, C. and Torii, K. U. (2012). Direct interaction of ligand-receptor pairs specifying stomatal patterning. *Genes Dev.* **26**, 126-136. doi:10.1101/gad.179895.111

Liu, T., Ohashi-Ito, K. and Bergmann, D. C. (2009). Orthologs of Arabidopsis thaliana stomatal bHLH genes and regulation of stomatal development in grasses. *Development* **136**, 2265-2276. doi:10.1242/dev.032938

Lu, J., He, J., Zhou, X., Zhong, J., Li, J. and Liang, Y. K. (2019). Homologous genes of epidermal patterning factor regulate stomatal development in rice. *J. Plant Physiol.* **234-235**, 18-27. doi:10.1016/j.jplph.2019.01.010

Pfaffl, M. W. (2001). A new mathematical model for relative quantification in real-time RT-PCR. *Nucleic Acids Res.* **29**, e45. doi:10.1093/nar/29.9.e45

Raissig, M. T., Abrash, E., Bettadapur, A., Vogel, J. P. and Bergmann, D. C. (2016). Grasses use an alternatively wired bHLH transcription factor network to establish stomatal identity. *Proc. Natl. Acad. Sci. USA* **113**, 8326-8331. doi:10.1073/pnas.1606728113

Raissig, M. T., Matos, J. L., Anleu Gil, M. X., Kornfeld, A., Bettadapur, A., Abrash, E., Allison, H. R., Badgley, G., Vogel, J. P., Berry, J. A. et al. (2017). Mobile MUTE specifies subsidiary cells to build physiologically improved grass stomata. *Science* **355**, 1215-1218. doi:10.1126/science.aal3254

Shaw, L. M., Turner, A. S. and Laurie, D. A. (2012). The impact of photoperiod insensitive Ppd-1a mutations on the photoperiod pathway across the three genomes of hexaploid wheat (Triticum aestivum). *Plant J.* **71**, 71-84. doi:10.1111/j.1365-313X.2012.04971.x

Sugano, S. S., Shimada, T., Imai, Y., Okawa, K., Tamai, A., Mori, M. and Hara-Nishimura, I. (2010). Stomagen positively regulates stomatal density in Arabidopsis. *Nature* **463**, 241-244. doi:10.1038/nature08682

Takata, N., Yokota, K., Ohki, S., Mori, M., Taniguchi, T. and Kurita, M. (2013). Evolutionary relationship and structural characterization of the EPF/EPFL gene family. *PLoS ONE* **8**, e65183. doi:10.1371/journal.pone.0065183

Tameshige, T., Okamoto, S., Lee, J. S., Aida, M., Tasaka, M., Torii, K. U. and Uchida, N. (2016). A secreted peptide and its receptors shape the auxin response pattern and leaf margin morphogenesis. *Curr. Biol.* **26**, 2478-2485. doi:10.1016/j.cub.2016.07.014

Tamnanloo, F., Damen, H., Jangra, R. and Lee, J. S. (2018). MAP KINASE PHOSPHATASE1 controls cell fate transition during stomatal development. *Plant Physiol.* **178**, 247-257. doi:10.1104/pp.18.00475

Uchida, N., Lee, J. S., Horst, R. J., Lai, H. H., Kajita, R., Kakimoto, T., Tasaka, M. and Torii, K. U. (2012). Regulation of inflorescence architecture by intertissue layer ligand-receptor communication between endodermis and phloem. *Proc. Natl. Acad. Sci. USA* **109**, 6337-6342. doi:10.1073/pnas.1117537109

Uchida, N. and Tasaka, M. (2013). Regulation of plant vascular stem cells by endodermis-derived EPFL-family peptide hormones and phloem-expressed ERECTA-family receptor kinases. *J. Exp. Bot.* **64**, 5335-5343. doi:10.1093/jxb/ert196

Wang, H., Guo, S., Qiao, X., Guo, J., Li, Z., Zhou, Y., Bai, S., Gao, Z., Wang, D., Wang, P. et al. (2019). BZU2/ZmMUTE controls symmetrical division of guard mother cell and specifies neighbor cell fate in maize. *PLoS Genet.* **15**, e1008377. doi:10.1371/journal.pgen.1008377

Wu, Z., Chen, L., Yu, Q., Zhou, W., Gou, X., Li, J. and Hou, S. (2019). Multiple transcriptional factors control stomata development in rice. *New Phytol.* **223**, 220-232. doi:10.1111/nph.15766

Yin, X., Biswal, A. K., Dionora, J., Perdigon, K. M., Balahadia, C. P., Mazumdar, S., Chater, C., Lin, H. C., Coe, R. A., Kretzschmar, T. et al. (2017). CRISPR-Cas9 and CRISPR-Cpf1 mediated targeting of a stomatal developmental gene EPFL9 in rice. *Plant Cell Rep.* **36**, 745-757. doi:10.1007/s00299-017-2118-z

Zuo, J., Niu, Q.-W. and Chua, N.-H. (2000). Technical advance: an estrogen receptor-based transactivator XVE mediates highly inducible gene expression in transgenic plants. *Plant J.* **24**, 265-273. doi:10.1046/j.1365-313x.2000.00868.x